

# Optical creation and temperature stability of the hidden charge density wave state in $1T\text{-TaS}_{2-x}\text{Se}_x$

L. Stojchevska,<sup>1</sup> P. Šutar,<sup>1</sup> E. Goreshnik,<sup>2</sup> D. Mihailovic,<sup>1,3</sup> and T. Mertelj<sup>1,3</sup>

<sup>1</sup>*Complex Matter Dept., Jozef Stefan Institute, Jamova 39, Ljubljana, SI-1000, Ljubljana, Slovenia*

<sup>2</sup>*Dept. of Inorganic Chemistry and Technology, Jozef Stefan Institute, Jamova 39, 1000 Ljubljana, Slovenia*

<sup>3</sup>*Center of Excellence on Nanoscience and Nanotechnology-Nanocenter (CENN Nanocenter), Jamova 39, 1000 Ljubljana, Slovenia*

The femtosecond transient optical spectroscopy is employed to study the relaxation dynamics of the equilibrium and hidden metastable charge-density-wave states in single crystals of  $1T\text{-TaS}_{2-x}\text{Se}_x$  as a function of the Se doping  $x$ . Similarly to pristine  $1T\text{-TaS}_2$ , the transition to a hidden phase is observed at low temperature after a quench with a single 50 fs laser pulse, in the commensurate Mott phase up to  $x = 0.6$ . The photo-induced hidden-phase formation is accompanied by a notable change in the coherent phonon spectra, and particularly the collective amplitude mode. While the stability of the hidden phase with increased temperatures is only slightly dependent of the Se content the hidden-phase creation-threshold fluence strongly increases with the Se content from 1 to  $\sim 4 \text{ mJ/cm}^2$ .

## INTRODUCTION

The interplay of different degrees of freedom shapes the manifold of emergent electronic and structural ordered phases in low-dimensional systems with competing interactions. A marked example is the class of non-semiconducting layered transition-metal dichalcogenides.[1] In this class  $1T\text{-TaS}_2$  is of particular interest due to the presence of a meta-stable hidden charge-density-wave state induced by short strongly-nonequilibrium optical[2] or electrical[3–5] excitations.

In equilibrium the pristine  $1T\text{-TaS}_2$  shows a series of electronic phase transitions upon cooling from high temperature.[6] First, at  $T_{\text{IC}} = 550 \text{ K}$  a transition to an incommensurate CDW (IC) phase is observed. With further cooling a first order transition to a nearly commensurate (NC) phase at  $T_{\text{NC}} = 350 \text{ K}$  results in formation of star-shaped-polaron clusters. Below  $T_{\text{C}}=183 \text{ K}$  the system undergoes a first-order lock-in transition into a commensurate (C) phase where the polarons order commensurately with the underlying atomic lattice. Concurrently, after Brillouin zone folding due to the enlarged unit cell, the resulting narrow half-filled Ta  $5d$  valence band splits due to the electronic correlations forming a  $\sim 300 \text{ meV}$  Mott insulator gap.[7, 8] Upon heating the C phase an additional trigonal (T) phase is observed between the C and NC phases in the range  $T_{\text{T}} = 220 \text{ K} < T < 280 \text{ K}$ . The C Mott state can be suppressed by pressure[9] or chemical doping[10] leading to the superconducting[11, 12] ground state.

The nonequilibrium dynamics of this compound have been under intensive investigation recently[2, 13–18], leading to the discovery[2] of the low-temperature metastable hidden (H) phase. The phase forms under strongly nonequilibrium conditions on a short timescale[19] and at low  $T$  the H phase is practically stable[2, 3]. With increasing  $T$  the characteristic relaxation time,  $\tau_{\text{H}}$ , shows activated behavior  $\tau_{\text{H}}^{-1} \propto \exp(-T_{\text{A}}/T)$ , where  $T_{\text{A}}$  depends on the in-plane strain[3]. In all-optical transient

reflectivity experiments in bulk samples  $\tau_{\text{H}}$  drops to the single scan timescale of  $\sim 30$  minutes at  $T \sim 70 \text{ K}$ . [2, 3] From the point of view of possible memory applications it would be desirable to improve the stability of the H state at higher  $T$ . Furthermore, the origin of metastability is still not fully understood, and it is thus of importance to investigate the influence of different external control parameters on its properties.

In the present case, we introduce isovalent Se substitution for S:  $1T\text{-TaS}_{2-x}\text{Se}_x$ , which exerts a chemical strain and introduces disorder. The introduction of the chemical strain and disorder strongly alters the electronic ground state of  $1T\text{-TaS}_{2-x}\text{Se}_x$ . [11, 12] With increasing  $x$  the the hysteresis related to the NC-C-T phase transitions broadens, with the C phase being pushed to lower  $T$  on cooling up to  $x \sim 0.8$ , whereafter the C Mott-insulating ground state is suppressed and the superconducting ground state appears.[11, 12]. The broader hysteresis at low doping suggests that the doping increases the free-energy barriers between the C, NC and T phases in addition to the suppression of the the insulating Mott state. Since a high enough free-energy barrier is crucial for the stability of the metallic H state we therefore investigated the influence of the Se doping on its formation threshold and stability.

Recently, the collective mode spectral shifts in  $1T\text{-TaS}_2$  were investigated both in equilibrium and in the metastable H and T states over a large range of temperatures.[19] Shifts in the collective mode frequency, which presumably arise from changes of electronic structure accompanying the transition to the H state, were shown to be a useful fingerprint signature of the H state. Here we use this to investigate the stability of the H state in  $1T\text{-TaS}_{2-x}\text{Se}_x$  with different  $x$ .

In the ultrafast transient reflectivity response the low frequency-phonon and collective mode frequencies are easily characterized by analysing the coherent transient response. [2, 19] We therefore employ the ultrafast transient reflectivity spectroscopy to  $1T\text{-TaS}_{2-x}\text{Se}_x$  ( $x = 0$ ,

0.15, 0.2, 0.5 and 0.6) single crystals before and after strong laser pulse photoexcitation to study the influence of the Se doping on the formation and temperature stability of the H-phase.

## EXPERIMENTAL

Single crystals of  $1T\text{-TaS}_{2-x}\text{Se}_x$  were grown by means of the chemical transport reaction with iodine as the transport agent. Appropriate reaction amounts of Ta, S and Se powders were put together with a small amount of  $\text{I}_2$  into evacuated quartz ampules and placed into a three-zone temperature gradient furnace. The crystal growth was achieved by setting the temperature gradient across the ampules to  $1000^\circ\text{C}\text{--}800^\circ\text{C}$  for 216 hours. Finally, ampules were quenched into water.

The Se content was determined by means of the standard energy-dispersive X-ray spectroscopy (EDS). For the optical measurements the characterized crystals were mounted on a cold finger of a liquid-He flow optical cryostat equipped with  $\text{CaF}_2$  windows and cleaved to expose fresh surface.

The optical pump-probe experiments were performed using a train of 50 fs laser pulses at 800 nm from a Ti:Sapphire laser system at a 250-kHz repetition rate. In order to ensure minimal heating and avoid switching into the H-phase the pump and probe fluences were kept constant during all measurements and estimated to be  $\mathcal{F}_p = 15 \mu\text{J}/\text{cm}^2$  and  $\mathcal{F}_{pr} = 0.5 \mu\text{J}/\text{cm}^2$  for the pump and probe pulses, respectively.

For switching into the H-phase an additional single laser pulse at 800 nm with fluence  $\mathcal{F}_{sw} = 1\text{--}5 \text{ mJ}/\text{cm}^2$  was picked from the pulse train by means of an acousto-optical modulator driven by a programmable waveform generator.

## RESULTS

In Fig. 1 we plot the characteristic transient reflectivity transients ( $\Delta R/R$ ) in the the C, H and NC phases in the  $x = 0.2$  sample together with the Fourier transform amplitude (FTA) spectra. The C and NC phases differ strongly in the shape and the amplitude of the transients. To determine  $T_C$  and  $T_T$  we first measured the  $T$ -dependence of the transients during a cooling-warming cycle between 300 K and  $\sim 70\text{K}$ . In Fig. 2 we show the normalized amplitude of the transients. Contrary to Refs. [10, 11] we observe a weak increase of  $T_C$  with increasing  $x$  while  $T_T$  and the broadening of the hysteresis show a similar trend.

We further analyse the  $T$ -dependent transients using the displacive coherent excitation (DCE) model[19–21]. Contrary to  $x = 0$  [19], where four modes were necessary to completely describe the lineshape in the vicinity of the 2.45-THz amplitude (AM) mode, using only two modes at  $\sim 2.45 \text{ THz}$  and  $\sim 2.1 \text{ THz}$  together with the initial

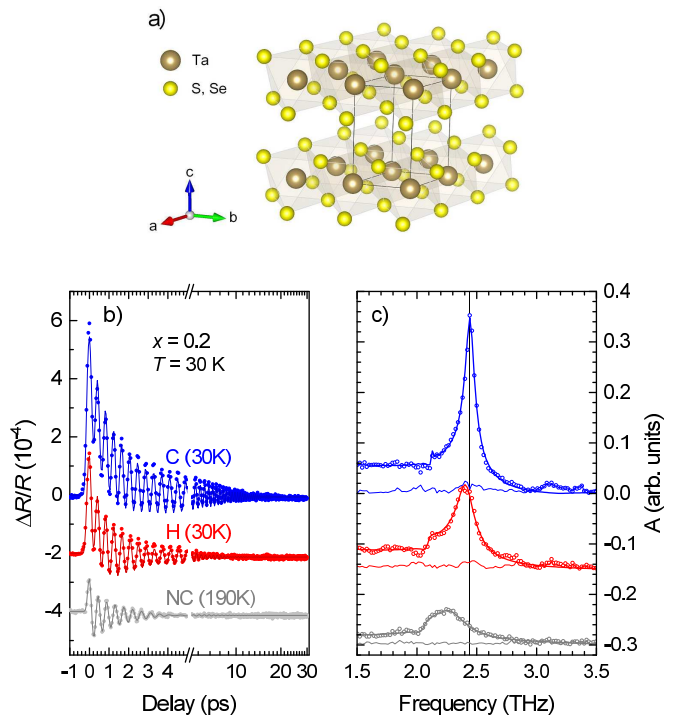


Figure 1. (a) The crystal structure of  $1T\text{-TaS}_{2-x}\text{Se}_x$ . Transient reflectivity in different phases (c) with the corresponding FTA spectra (d). The thick lines are DCE fits. The thin lines in (d) correspond to the fit residua.

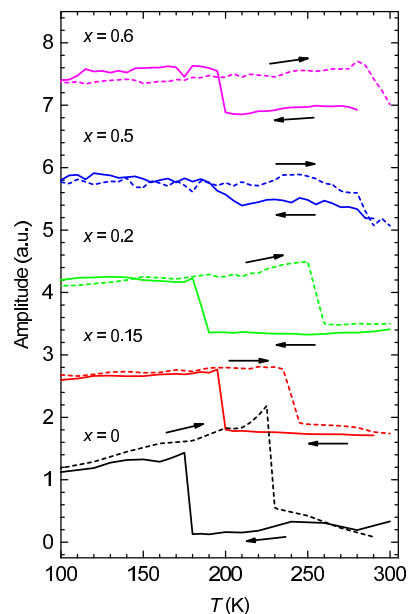


Figure 2. Temperature dependence of the normalized transient reflectivity amplitude for different  $x$ . The data for different  $x$  are shifted vertically while the arrows indicate cooling and warming scans.

exponential relaxation enabled a fair fit to the data (see Fig. 1). The  $T$ -dependence of selected fit parameters for  $x = 0.2$  sample is shown in Fig. 3. The 2.1-THz mode

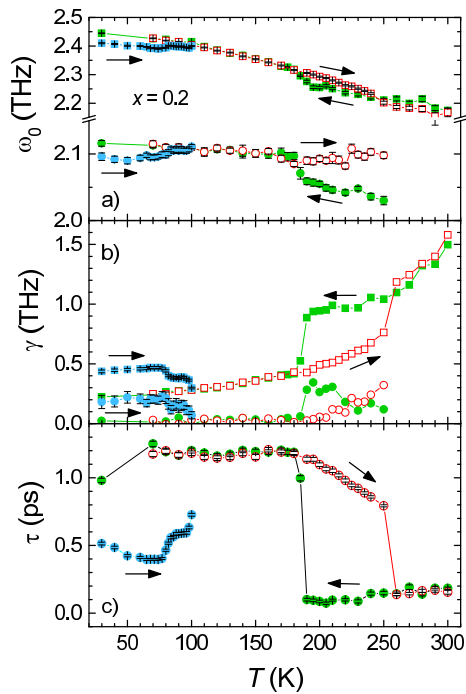


Figure 3. Temperature dependence of the modes frequency,  $\omega_0$ , damping,  $\gamma$ , and the initial relaxation time,  $\tau$ , from the DCE fit for the  $x = 0.2$  sample. Arrows indicate colling/warming cycles. The blue symbols correspond to the warming scan in the H-phase after application of an above-threshold optical switching pulse at  $T = 30$  K.

could be unambiguously fitted only below  $T \sim 250$  K due to weaker intensities and strong broadening of the modes in the NC and T phases. Apart from the frequencies, the mode damping and the initial relaxation decay time  $\tau$ , both show notable differences in different CDW phases.

Next, we checked for the presence of the H-phase and determine the switching fluence at  $T = 30$  K by measuring a series of the low-fluence  $\Delta R/R$  transients after an exposure to a single switching pulse of increasing fluence. An example sequence of the FTA spectra with increasing  $\mathcal{F}_{\text{SW}}$  in the  $x = 0.2$  sample are shown in Fig. 4. The H phase is characterized mainly by the softening of the strongest coherent mode from  $\sim 2.45$  THz in the C phase to  $\sim 2.40$  THz (at  $T = 30$  K). The onset of the characteristic AM mode spectral weight transfer[2] is observed at  $\mathcal{F}_{\text{SW}} = 2.3$  mJ/cm<sup>2</sup>. The switching is complete above  $\mathcal{F}_{\text{SW}} = 2.7$  mJ/cm<sup>2</sup>. In the intermediate  $\mathcal{F}_{\text{SW}}$ -interval the spectral shape indicates incomplete switching with the presence of both, C and H phases. The behavior is similar for all studied Se contents with the C- and H-phase spectra and the corresponding threshold fluences,  $\mathcal{F}_{\text{H}}$ , shown in Fig. 5 and Table I. Here,  $\mathcal{F}_{\text{H}}$  is defined as the minimal fluence where the completed spectral change is observed and it strongly increases with increasing  $x$ .

Once we had driven the system into the H-phase, we investigated the  $T$  dependence of the reflectivity transients in the H-phase. In these experiments, the H-phase

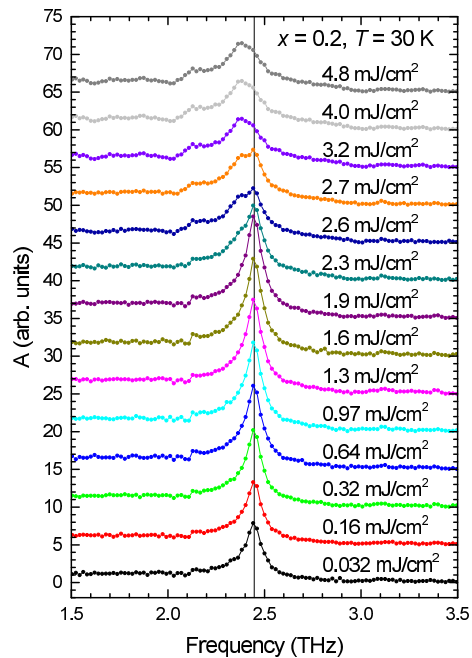


Figure 4. The switching-pulse fluence dependence of the low-fluence transient reflectivity FTA spectra at 30 K for  $x = 0.2$  sample.

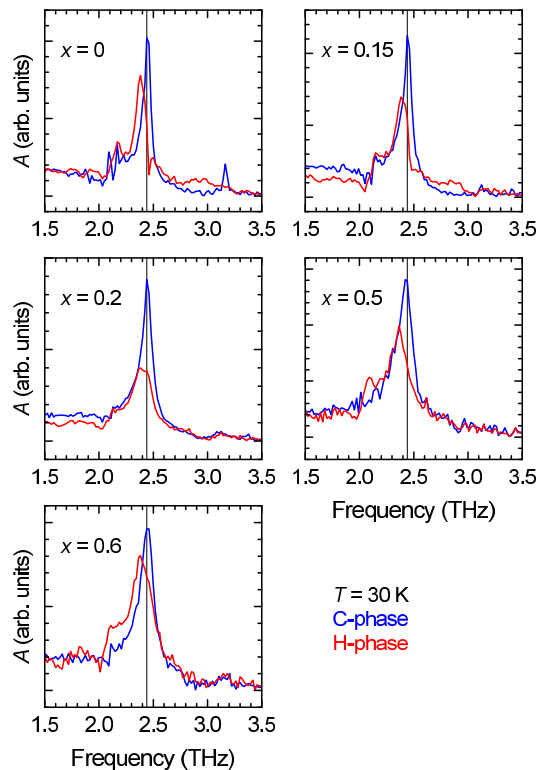


Figure 5. Reflectivity transients FTA spectra in the C and H-phase at  $T = 30$  K for different Se doping levels,  $x$ .

transition was first triggered by the above-threshold fluence switching pulse at  $T = 30$  K. Then the  $\Delta R/R$  tran-

$x$	$T_C$	$T_T$	$\mathcal{F}_H$ (@ 30 K)	$T_H$
0	180 K	225 K	1 mJ/cm <sup>2</sup>	80 K
0.15	200 K	240 K	1.5 ± 0.1 mJ/cm <sup>2</sup>	80 K
0.2	185 K	255 K	3 ± 0.2 mJ/cm <sup>2</sup>	80 K
0.5	200 K	280 K	4 ± 0.4 mJ/cm <sup>2</sup>	95 K
0.6	200 K	290 K	3.6 ± 0.4 mJ/cm <sup>2</sup>	85 K

Table I. The transition temperatures to/from the C state upon cooling ( $T_C$ ) and warming ( $T_T$ ), the threshold fluence,  $\mathcal{F}_H$ , for switching into the H-phase at  $T = 30$  K and the highest temperature  $T_H$  up to which the H-phase persists on the timescale of the pump-probe scan ( $\sim 30$  min) for different Se dopings.

sients were recorded using a weak pump-probe sequence at an increasing  $T$  sequence until the C-phase transient response was observed.

The  $T$ -dependence of the selected DCE-fit parameters in the H-phase for the  $x = 0.2$  sample is also shown in Fig. 3. While the frequencies of both modes soften in the H-phase, the modes decay faster (damping,  $\gamma$ , increases) and the initial exponential relaxation time,  $\tau$ , decreases. With increasing  $T$  the strongest H-phase mode shows a similar softening with increasing  $T$  as in the C-phase (see also Fig. 6) until, at  $T_H$ , a recovery of the C-phase transient response is observed.<sup>1</sup>

$T_H \sim 80$  K does not show a strong variation with  $x^2$  except for  $x = 0.5$  with  $T_H \sim 95$  K (Table I). In the  $x = 0.5$  sample we observe also a slightly softer AM mode in the C-phase together with the softer corresponding mode in the H-phase while for other dopings the frequency shift is observed only in the H-phase.

## DISCUSSION

Contrary to earlier results[10, 11] our samples do not show a significant decrease of  $T_C$  with increasing  $x$ . Since the NC $\rightarrow$ C transition is of first order the pinning of the CDW in the NC phase by the Se disorder can play a significant role in supercooling the NC phase. Since the disorder can be sample dependent the difference may be attributed to the sample dependent disorder. On the other hand, our measurements were done under a weak continuous pump-probe optical excitation that can contribute to depinning and helps to trigger the transition at higher  $T$ .

Overall, the observed effect of Se substitution on the H phase is two fold. Firstly, the transition temperature  $T_H$

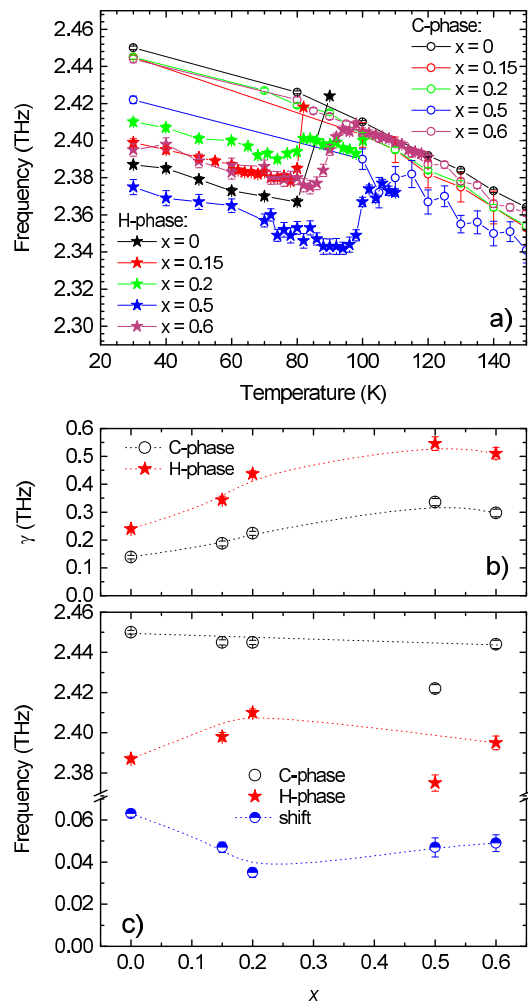


Figure 6. (a) Temperature dependence of the 2.40-THz mode frequency on warming after switching into the H-phase at 30K. The empty symbols refer to the frequency in the C phase. (b) Se doping dependence of the 2.4(5)-THz mode damping and (c) the frequency at  $T = 30$  K in the C and H phases. The dotted lines are guide lines. The errorbars correspond to the errors obtained from the DCE-fit.

increases slightly or not at all, with increasing  $x$  as a result of increasing tensile strain[11] exerted by the larger Se substitution. We can qualitatively compare the chemical strain effect of Se ion substitution with in-plane differential strain experiments with thin crystals of 1T-TaS<sub>2</sub> on different substrates, where a tensile strain on cooling was found to empirically increase  $T_H$ . The two trends thus agree qualitatively.

The second effect is that the threshold fluence increases with increasing  $x$ . Pinning by the Se dopants would be expected to have an opposite effect in stabilizing the domain structure created in the switching process. Another possibility is that the absorption coefficient is changing with Se doping, changing the effective carrier density. The photon absorption near 1.5 eV is related to a charge-transfer excitation between metal and chalcogen, and is

<sup>1</sup> Since the stability time,  $\tau_H$ , of the H-phase strongly depends on  $T$  [3]  $T_H$  is set by the timescale of experiment[19], that was  $\sim 30$  minutes in the present case. On shorter timescale the H-phase can be readily observed at much higher  $T$ . [19]

<sup>2</sup> In the  $x = 0.2$  sample we observe a two step recovery of the C-phase with the dominant recovery of the spectral shape at  $\sim 80$  K with the H-phase signature up to  $\sim 100$  K.

close to the absorption edge for this transition. It is therefore conceivable that the chalcogen substitution can have an effect on the imaginary part of the dielectric constant in this region. Unfortunately, presently ellipsometric data are not available to confirm or disprove this hypothesis. The effect of disorder may also have an influence if doping is associated with traps (e.g. on interstitials), thus reducing the photoinduced carrier density. A threefold increase in threshold fluence would require a significant number of traps, which we consider unlikely.

The frequency of the AM in the C phase does not show a systematic  $x$ -dependence while the corresponding mode frequency in the H-phase shows a small,<sup>3</sup> but detectable, dependence [see Fig. 6 c)]. The absence of the shift in the C-phase indicates that the AM mode eigenvector does not include significant (S,Se) site displacements. Since the corresponding mode observed in the H-phase hardens slightly with increasing  $x$  the shift can not be related to the larger Se mass. Considering that the broadening of the modes is the most likely inhomogeneous and  $\gamma$  is an order of magnitude larger [see Fig. 6 b)] than the shift the origin of the shift can be attributed to a doping dependence of the Se inhomogeneity.

Moreover, in the  $x = 0.5$  sample a notable softening of  $\sim 0.03$  THz in comparison to the  $x \neq 0.5$  samples is observed in both phases. This suggests a possibility of a Se ordering at this doping since  $x = 0.5$  corresponds to a commensurate 25% filling of the triangular (S,Se) site lattice. The ordering, however, can not be long range since the mode linewidth is the largest at this doping. Nevertheless, the slight increase of the the H-phase sta-

bility at  $x = 0.5$  could be tentatively linked to enhanced pinning of the H-phase domain walls by partially ordered rows of Se ions.

## CONCLUSIONS

We demonstrated a successful transition of 1T-TaS<sub>2-x</sub>Se<sub>x</sub> system to the hidden photo-induced state over a major portion of the Mott-phase region ( $x \leq 0.6$ ). The H-state transition is triggered by an ultrafast laser quench similarly to the pristine 1T-TaS<sub>2</sub>,<sup>[2]</sup> but at fluences that significantly increase with increasing  $x$  from  $\mathcal{F}_H \sim 1$  mJ/cm<sup>2</sup> at  $x = 0$  to  $\mathcal{F}_H \sim 4$  mJ/cm<sup>2</sup> at  $x = 0.5$ . The high temperature stability of the H-phase is not significantly influenced by the Se doping despite a much larger effect on the stability of the equilibrium C phase. An exception is  $x = 0.5$  Se doping where the slight increase of the the H-phase stability concurrent with the AM mode softening could be tentatively linked to partial Se-ion ordering.

## ACKNOWLEDGMENTS

The authors acknowledge the financial support of Slovenian Research Agency (research core funding No-P1-0040) and European Research Council Advanced Grant TRAJECTORY (GA 320602) for financial support. L. S. would also like to acknowledge supported by MIZŠ&ESS funds, ULTRA-MEM-Device project, 2014-2015.

- 
- [1] J. A. Wilson, F. Di Salvo, and S. Mahajan, *Advances in Physics* **24**, 117 (1975).
- [2] L. Stojchevska, I. Vaskivskiy, T. Mertelj, P. Kusar, D. Svetin, S. Brazovskii, and D. Mihailovic, *Science* **344**, 177 (2014).
- [3] I. Vaskivskiy, J. Gospodaric, S. Brazovskii, D. Svetin, P. Sutar, E. Goreshnik, I. A. Mihailovic, T. Mertelj, and D. Mihailovic, *Science advances* **1**, e1500168 (2015).
- [4] M. J. Hollander, Y. Liu, W.-J. Lu, L.-J. Li, Y.-P. Sun, J. A. Robinson, and S. Datta, *Nano letters* **15**, 1861 (2015).
- [5] I. Vaskivskiy, I. Mihailovic, S. Brazovskii, J. Gospodaric, T. Mertelj, D. Svetin, P. Sutar, and D. Mihailovic, *Nature communications* **7**, 11442 (2016).
- [6] R. Thomson, B. Burk, A. Zettl, and J. Clarke, *Physical Review B* **49**, 16899 (1994).
- [7] P. Fazekas and E. Tosatti, *Philosophical Magazine B* **39**, 229 (1979).
- [8] B. Dardel, M. Grioni, D. Malterre, P. Weibel, Y. Baer, and F. Lévy, *Phys. Rev. B* **46**, 7407 (1992).
- [9] B. Sipos, A. F. Kusmartseva, A. Akrap, H. Berger, L. Forró, and E. Tutiš, *Nat. Mater.* **7**, 960 (2008).
- [10] F. Di Salvo, J. Wilson, B. Bagley, and J. Waszczak, *Phys. Rev. B* **12**, 2220 (1975).
- [11] Y. Liu, R. Ang, W. Lu, W. Song, L. Li, and Y. Sun, *Appl. Phys. Lett.* **102**, 192602 (2013).
- [12] R. Ang, Y. Miyata, E. Ieki, K. Nakayama, T. Sato, Y. Liu, W. Lu, Y. Sun, and T. Takahashi, *Phys. Rev. B* **88**, 115145 (2013).
- [13] J. Demsar, L. Forró, H. Berger, and D. Mihailovic, *Phys. Rev. B* **66**, 041101 (2002).
- [14] N. Dean, J. C. Petersen, D. Fausti, R. I. Tobey, S. Kaiser, L. Gasparov, H. Berger, and A. Cavalleri, *Phys. Rev. Lett.* **106**, 016401 (2011).
- [15] L. Perfetti, P. Loukakos, M. Lisowski, U. Bovensiepen, H. Berger, S. Biermann, P. Cornaglia, A. Georges, and M. Wolf, *Phys. Rev. Lett.* **97**, 067402 (2006).
- [16] K. Haupt, M. Eichberger, N. Erasmus, A. Rohwer, J. Demsar, K. Rossnagel, and H. Schwoerer, *Phys. Rev. Lett.* **116**, 016402 (2016).
- [17] C. Laulhé, T. Huber, G. Lantz, A. Ferrer, S. O. Mariager, S. Gröbel, J. Rittmann, J. A. Johnson, V. Esposito, A. Lübcke, L. Huber, M. Kubli, M. Savoini, V. L. R. Jacques, L. Cario, B. Corraze, E. Janod, G. Ingold, P. Beaud, S. L. Johnson, and S. Ravy, *Phys. Rev. Lett.* **118**, 247401 (2017).

<sup>3</sup> An order of magnitude smaller than  $\gamma$ .

- [18] M. Ligges, I. Avigo, D. Golež, H. Strand, Y. Beyazit, K. Hanff, F. Diekmann, L. Stojchevska, M. Källäne, P. Zhou, *et al.*, *Physical Review Letters* **120**, 166401 (2018).
- [19] J. Ravnik, I. Vaskivskyi, T. Mertelj, and D. Mihailovic, *Physical Review B* **97**, 075304 (2018).
- [20] H. Zeiger, J. Vidal, T. Cheng, E. Ippen, G. Dresselhaus, and M. Dresselhaus, *Physical Review B* **45**, 768 (1992).
- [21] L. Stojchevska, M. Borovšak, P. Foury-Leylekian, J.-P. Pouget, T. Mertelj, and D. Mihailovic, *Physical Review B* **96**, 035429 (2017).